Johannes Böhm, Robert Heinkelmann, and Harald Schuh

Short Note:
A Global Model of Pressure and Temperature for Geodetic Applications

Journal of Geodesy
doi:10.1007/s00190-007-0135-3

2007a

Short Note:
A Global Model of Pressure and Temperature for Geodetic Applications

Johannes Böhm, Robert Heinkelmann, and Harald Schuh

Abstract

The empirical model GPT (Global Pressure and Temperature), which is based on spherical harmonics up to degree and order nine, provides pressure and temperature at any site in the vicinity of the Earth's surface. It can be used for geodetic applications such as the determination of a priori hydrostatic zenith delays, reference pressure values for atmospheric loading, or thermal deformation of Very Long Baseline Interferometry (VLBI) radio telescopes. Input parameters of GPT are the station coordinates and the day of the year, thus also allowing one to model the annual variations of the parameters. As an improvement compared to previous models, it reproduces the large pressure anomaly over Antarctica, which can cause station height errors in the analysis of space geodetic data of up to one centimetre if not considered properly in troposphere modelling. First tests at selected geodetic observing stations show that the pressure biases considerably decrease when using GPT instead of the very simple approaches applied in various Global Navigation Satellite Systems (GNSS) software packages so far. GPT also provides an appropriate model of the annual variability of global temperature.

Keywords: GNSS, VLBI, neutral atmosphere delays

1 Introduction

In the analysis of Global Navigation Satellite System (GNSS) and Very Long Baseline Interferometry (VLBI) observations, accurate a priori hydrostatic zenith delays must be used. Preferably, they are determined from pressure values recorded at the sites (Saastamoinen 1972), but they can also be derived from numerical weather models (NWM), although with some loss of accuracy. For example, hydrostatic zenith delays are provided with the coefficients of the NWM-based Vienna Mapping Function 1 (Boehm et al. 2006a). If neither of these two data streams is accessible, a standard model for the pressure is often used. To provide precise and un-biased global pressure values, we have derived the empirical model

GPT (Global Pressure and Temperature) which describes the annual variation of the pressure at the Earth surface and which agrees with mean pressure values so that no systematic station height errors are introduced.
The pressure values calculated from GPT can also be entered into atmosphere pressure loading models as reference pressure, whereas the temperature values can be used for determining annual thermal deformations of radio telescopes (or for buildings with GNSS antennas on top of them) or as reference temperatures for these thermal deformations, respectively. Finally, as a by-product, GPT yields rough estimates for global geoid undulations.

2 Determination of GPT

In terms of mathematics and the underlying meteorological data, the determination of GPT is similar to the development of the empirical Global Mapping Function (GMF) (Boehm et al. 2006b), i.e., it is based on three years (September 1999 to August 2002) of 15° x 15° global grids of monthly mean profiles for pressure and temperature from the ECMWF (European Centre for Medium-Range Weather Forecasts) 40 years reanalysis data (ERA40, Uppala et al. 2005). The corresponding grid of orthometric heights H of the Earth surface with respect to mean sea level is also available from the ECMWF.
In a first step, for each vertical profile, the pressure and temperature values are determined for the Earth surface by interpolating exponentially and linearly, respectively. Then, the pressure values p on the Earth surface at height h are reduced to pressure values p_r at mean sea level h_r (Eq. 1, Berg 1948) and a linear decrease of temperature T with height is assumed (Eq. 2).

$$p = p_r \cdot \left(1 - 0.0000226 \cdot \left(h - h_r\right)\right)^{5.225} \tag{1}$$

$$dT/dh = -0.0065\,°C/m \tag{2}$$

Thus for each grid point 36 monthly mean values of pressure and temperature at mean sea level are available. For these two series the mean values, a_0, and the annual amplitudes, A, are estimated with the phase offset fixed to January 28 (Niell 1996) when *doy* is the day of the year.

(3) $$a = a_0 + A \cdot \cos\left(\frac{doy - 28}{365.25} \cdot 2\pi\right)$$

The residuals to this model are as large as 20 hPa for the pressure and 10 °C for the temperature at higher latitudes; they are significantly smaller at the equator, consistent with the meteorological variability (Fig. 1).

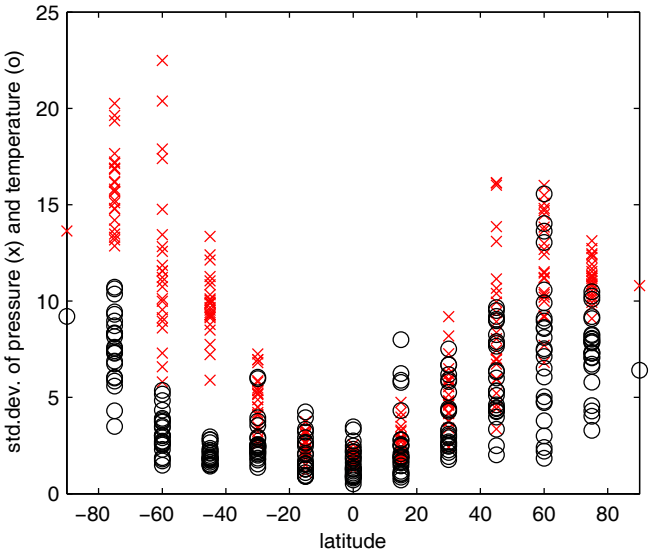

Figure 1. Standard deviation of residuals to the annual model for pressure [hPa] (x) and temperature [°C] (o) with respect to latitude.

In the next step, each of the four grids (mean values at mean sea level and annual amplitudes of pressure and temperature) is expanded into spherical harmonics up to degree and order nine (as an example see Eq. 4 for the grid of mean values, a_0). The P_{nm} are the Legendre polynomials (Heiskanen and Moritz 1967, p. 22), φ and λ are latitude and longitude, and A_{nm} and B_{nm} are the coefficients for degree n and order m which are determined within a least-squares adjustment.

(4) $$a_0 = \sum_{n=0}^{9} \sum_{m=0}^{n} P_{nm}(\sin\varphi) \cdot \left[A_{nm} \cos(m\lambda) + B_{nm} \sin(m\lambda)\right]$$

GPT uses Eq. (4) to derive the mean value, a_0, and a similar equation for amplitude, A, which are then entered into Eq. (3) together with the day of the year to get the pressure or the temperature at mean sea level. Constant reference values for pressure and temperature (yearly means) can be derived from Eq. (3) if (28 + 365.25/4) is used as day of the year. To determine

the pressure and temperature at the site, the orthometric height H should be used together with Eq. (1) and (2), respectively. However, since the orthometric heights of the stations are often not accessible for the user, GPT accepts ellipsoidal height as input. To accommodate this the geoidal undulations N from the EGM96 model (Lemoine et al. 1998) have been expanded into spherical harmonics up to degree and order nine and are used to transform the ellipsoidal heights h to orthometric heights H ($h = H + N$). The geoidal undulation N can be as large as 100 m (approximately 12 hPa); applying a rule of thumb (e.g. MacMillan and Ma 1994), an error of the pressure value of 12 hPa used in the troposphere model corresponds to a station height error of approximately 3 mm.

3 Validation of GPT

In the Bernese software package (BSW, Hugentobler et al. 2006) Eq. (1) by Berg (1948) is used together with the reference pressure p_r = 1013.25 hPa at the ellipsoid to determine the pressure p at the site which is then used to calculate the a priori hydrostatic zenith delay (Saastamoinen 1972). In the GAMIT software (King and Bock 2006) Eq. (5) by Hopfield (1969) is applied with the atmospheric temperature T_k = 293.16 K, the normal lapse rate of temperature with height α = 4.5 K/km, the gravity at the surface of the Earth g = 9.7867 m/s^2, the gas constant for dry air R = 0.287 kJ/K/kg, and also the reference pressure p_r = 1013.25 hPa at the ellipsoid.

$$p = p_r \cdot \left(\frac{T_k - \alpha \cdot h}{T_k} \right)^{(g/R\alpha)} \tag{5}$$

Fig. 2 shows by latitude band the mean values and standard deviations of the differences of pressure derived from GPT and pressure determined with the models by Berg and Hopfield (both assuming 1013.25 hPa at the ellipsoid). Most striking is the significant decrease of the pressure towards the South Pole which is modelled by GPT but cannot be accounted for by the models Berg and Hopfield because of two reasons: (1) Low mean sea level pressure is dominating at the coast of the Antarctica (Uppala et al. 2005); (2) Although the vertical gradient of the pressure is dependent on the temperature, the models by Berg and Hopfield (as implemented in GAMIT) imply constant values for the temperature and temperature lapse rates. This weakness is even more important for Antarctica because the heights can be as large as 3 km. GPT also uses a constant pressure gradient (Eq. 1) but the extrapolation of the

pressure gets started at the mean Earth surface and not at the ellipsoid as it is the case with the models by Berg and Hopfield. Similar differences as shown in Fig. 2 have also been found by Tregoning and Herring (2006).

A pressure difference of 40 hPa as shown in Fig. 2 for the South Pole causes an apparent station height change in the geodetic analysis of more than 10 mm. However, since the slope of the pressure differences towards the South Pole is so distinct and the difference of 40 hPa is so large, we performed an independent comparison with monthly mean local pressure measurements in 1998 at the South Pole provided by the NOAA (National Oceanic and Atmospheric Administration, U.S.A.). Fig. 3 shows these monthly mean values of observed pressure values together with GPT and the Berg model, and it clearly confirms the pressure anomaly shown in Fig. 2. As we want to confirm these results with other independent observations, i.e. not with data retrieved from the ECMWF, recorded pressure values have been extracted from the VLBI databases. Fig. 4 shows these meteorological observations for station O'Higgins in Antarctica (-63° latitude, -58° eastern longitude) in comparison with GPT and the Berg model from year 2000 until 2005. Additionally, surface pressure values from the ECMWF given at 6 hour time intervals are plotted. It is evident that the recorded values at the station agree well with data from the ECMWF and are well represented by GPT, but that the model by Berg (Eq. 1) assuming 1013.25 hPa on the ellipsoid differs by approximately -15 hPa. This pressure difference at O'Higgins between GPT and the model by Berg is different from the mean values per latitude shown in Fig. 1 because there is also a large variation with longitude in this region.

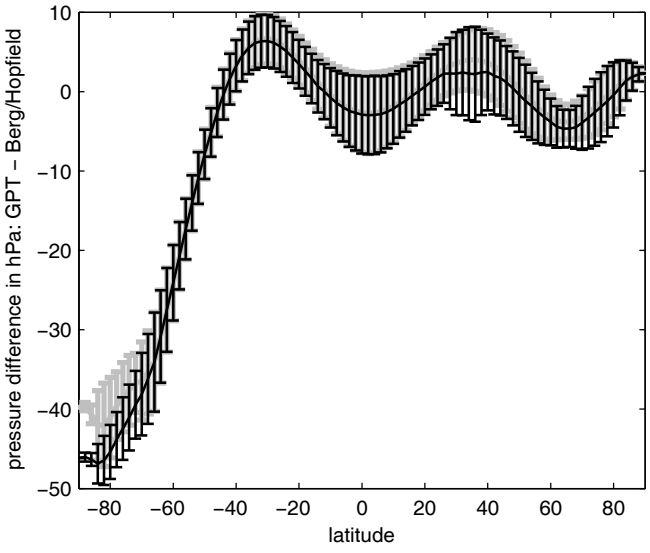

Figure 2. Pressure differences in hPa between GPT and the models by Berg (Eq. 1, grey error bars) and Hopfield (Eq. 3, black error bars) assuming 1013.25 hPa at the ellipsoid.

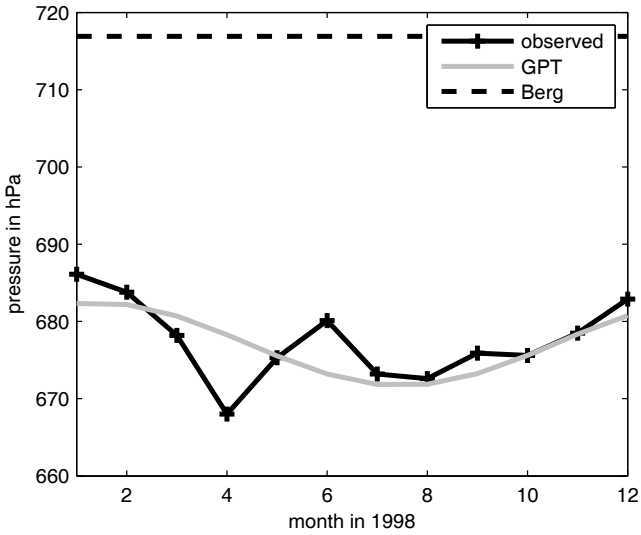

Figure 3. Monthly mean pressure values in 1998 observed at the South Pole (+), and the corresponding values from GPT (grey line) and the Berg model (dashed line).

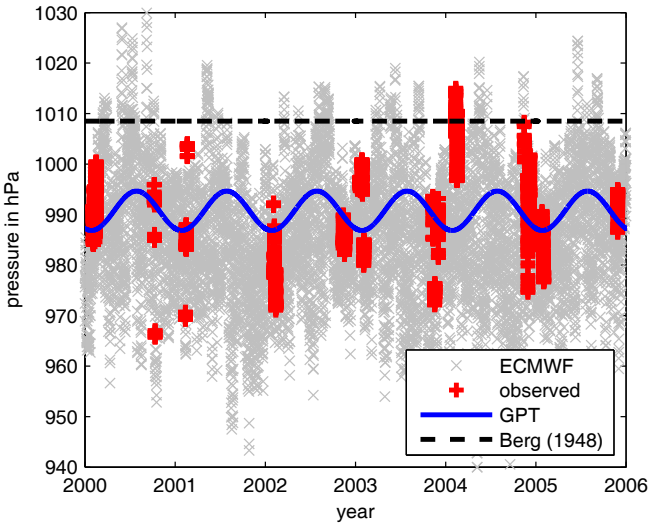

Figure 4. Pressure values for station O'Higgins in Antarctica from the ECMWF (x), pressure recordings at the radio telescope (+), GPT (-), and pressure determined with Eq. (1) (--).

Analogously, Fig. 5 shows the temperature values for O'Higgins. Unlike the pressure, there is a relatively large annual variation of the temperature which again is nicely represented by GPT.

Table 1 summarizes the biases and standard deviations between the recorded pressure and temperature values at six frequently observing VLBI radio telescopes and the modelled values for pressure from GPT and Eq. (1) and temperature from GPT and Eq. (2) (assuming a reference temperature of 15 °C at mean sea level). (It should be noted that the recorded pressure and temperature values are available only during the VLBI sessions, i.e. for about

one or two days per week.) Table 1 shows that the pressure bias is significantly reduced from Eq. (1) to GPT for four out of six stations. In particular the three largest biases get clearly smaller (Hartebeesthoek from 11.0 to 2.8 hPa, Kokee Park from 8.6 to 4.4 hPa, Wettzell from 10.8 to 2.7 hPa). The maximum bias for GPT is obtained at Algonquin Park with 5.7 hPa, which corresponds to a station height error of about 1.5 mm. On the other hand, there is no reduction of the standard deviation of the pressure, which is due to the fact that short term variations of the pressure (e.g. within a couple of days) far exceed the effect of annual pressure variations. This is different for the temperature where a clear improvement of the standard deviations is obtained if the annual variation is taken into account: As can be seen from the two last columns of Table 1, for three stations the standard deviations decrease by more than 40% with the new GPT model.

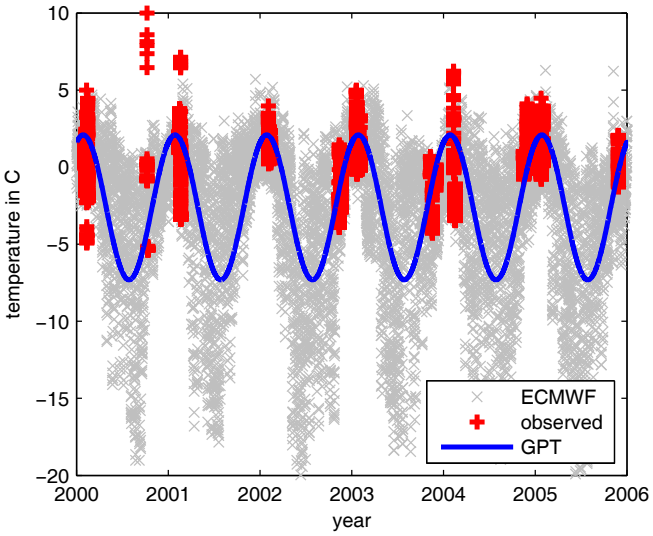

Figure 5. Temperature values for station O'Higgins in Antarctica from the ECMWF (x), temperature recordings at the radio telescope (+), and GPT (-).

Conclusions

It frequently happens in space-geodetic techniques data analyses that neither observed (recorded) pressure values nor values from a NWM are available to determine the hydrostatic zenith delays. In those instances we recommend the use of GPT for troposphere modelling in GNSS or VLBI analyses instead of taking simple models like the one given in Eq. (1). GPT can be easily implemented in any software package, and a combination of GPT with GMF (Boehm et al. 2006b) is useful. Because it is an empirical model, GPT can be used to define reference values for the pressure and temperature for other geodetic applications, such as

atmosphere loading or thermal deformations of VLBI radio telescopes. Future improvements of GPT might consider an increase of degree and order of the spherical harmonics expansion, however, such an update should be consistently done with an update of the Global Mapping Functions (GMF). GPT can be downloaded from http://www.hg.tuwien.ac.at/~ecmwf1 .

Table 1. Biases and standard deviations between pressure and temperature values recorded at VLBI radio telescopes in 2005, and those determined either with GPT or Eq. (1) and (2) (Berg, 1948). For the comparison of the temperatures in the last column, 15 °C is used as reference value at mean sea level.

	latitude [°]	pressure [hPa] rec. – GPT	pressure [hPa] rec. – Berg	temp. [°C] rec. – GPT	temp. [°C] rec. – Eq. 2
Algonquin Park	46	5.7 ± 7.4	2.9 ± 7.3	0.5 ± 7.2	-10.2 ± 13.6
Hartebeesthoek	-26	2.8 ± 3.4	11.0 ± 3.7	0.3 ± 6.2	8.8 ± 6.4
Kokee Park	22	4.4 ± 2.3	8.6 ± 2.3	-0.3 ± 2.6	6.5 ± 2.8
Ny-Ålesund	78	0.7 ± 12.9	-2.9 ± 12.7	0.0 ± 5.4	-20.3 ± 5.9
Westford	49	1.2 ± 7.4	-0.5 ± 7.4	2.3 ± 5.8	-4.9 ± 10.9
Wettzell	42	2.7 ± 7.1	10.8 ± 7.0	0.3 ± 4.8	-4.9 ± 8.4

Acknowledgement

The authors would like to thank the *Zentralanstalt für Meteorologie und Geodynamik* (ZAMG, Wien) for providing access to the data of the European Centre for Medium-Range Weather Forecasts and Arthur Niell for his helpful review.

References

Berg H (1948) Allgemeine Meteorologie. Dümmler Verlag, Bonn

Boehm J, B Werl, H Schuh (2006a) Troposphere mapping functions for GPS and very long baseline interferometry from European Centre for Medium-Range Weather Forecasts operational analysis data. J. Geophys. Res., 111, B02406, doi: 10.1029/2005JB003629

Boehm J, AE Niell, P Tregoning, H Schuh (2006b) The Global Mapping Function (GMF): A new empirical mapping function based on data from numerical weather model data. Geophys. Res. Lett., 33, L07304, doi: 10.1029/2005GL025546

Heiskanen WA, H Moritz (1967) Physical Geodesy. Freeman, San Francisco

Hopfield HS (1969) Two-quartic tropospheric refractivity profile for correcting satellite data, J. Geophys. Res., 74: 4487-4499

Hugentobler U, R Dach, P Fridez, and M Meindl (eds.) (2006) Bernese GPS Software Version 5.0, Astronomical Institute, University of Berne

King RW, Y Bock (2006) Documentation for the GAMIT GPS processing software Release 10.2, Mass. Inst. of Technol., Cambridge, MA

Lemoine FG, SC Kenyon, JK Factor, RG Trimmer, NK Pavlis, DS Chinn, CM Cox, SM Klosko, SB Luthcke, MH Torrence, YM Wang, RG Williamson, EC Pavlis, RH Rapp, TR Olson (1998) The development of the joint NASA GSFC and the National Imagery and Mapping Agency (NIMA) geopotential model EGM96. NASA/TP-1998-20681, NASA, Greenbelt

MacMillan DS, C Ma (1994) Evaluation of very long baseline interferometry atmospheric modeling improvements. J. Geophys. Res., 99(B1): 637-651

Niell AE (1996) Global mapping functions for the atmosphere delay at radio wavelengths. J. Geophys. Res., 101(B2): 3227-3246

Saastamoinen J (1972) Atmospheric correction for the troposphere and stratosphere in radio ranging of satellites. The use of artificial satellites for geodesy, Geophys. Monogr. Ser. 15, Amer. Geophys. Union, 274-251

Tregoning P, TA Herring (2006) Impact of a priori hydrostatic zenith delay errors on GPS estimates of station heights and zenith total delays. Geophys. Res. Letters, 33, L23303, doi:10.1029/2006GL027706

Uppala SM, PW Kållberg, AJ Simmons, U Andrae, V da Costa Bechtold, M Fiorino, JK Gibson, J Haseler, A Hernandez, GA Kelly, X Li, K Onogi, S Saarinen, N Sokka, RP Allan, E Andersson, K Arpe, MA Balmaseda, ACM Beljaars, L van de Berg, J Bidlot, N Bormann, S Caires, F Chevallier, A Dethof, M Dragosavac, M Fisher, M Fuentes, S Hagemann, E Hólm, BJ Hoskins, L Isaksen, PAEM Janssen, R Jenne, AP McNally, J-F Mahfouf, J-J Morcrette, NA Rayner, RW Saunders, P Simon, A Sterl, KE Trenberth, A Untch, D Vasiljevic, P Viterbo, and J Woollen (2005) The ERA-40 re-analysis, Quarterly Journal of the Royal Meteorological Society, 131, doi:10.1256/qj.04.176, pp. 2961-3012